HHS Public Access

Author manuscript

J Control Release. Author manuscript; available in PMC 2019 August 10.

Published in final edited form as:

J Control Release. 2018 August 10; 283: 135–142. doi:10.1016/j.jconrel.2018.05.033.

Remote control of movement disorders using a photoactive adenosine A_{2A} receptor antagonist

Jaume Taura[1,2], **Ernest G. Nolen**[3], **Gisela Cabré**[4], **Jordi Hernando**[4], **Lucia Squarcialupi**[5], **Marc López-Cano**[1,2], **Kenneth A. Jacobson**[5], **Víctor Fernández-Dueñas**[1,2], and **Francisco Ciruela**[1,2]

[1]Unitat de Farmacologia, Departament Patologia i Terapéutica Experimental, Facultat de Medicina, IDIBELL, Universitat de Barcelona, L'Hospitalet de Llobregat, Spain

[2]Institut de Neurociències, Universitat de Barcelona, Spain

[3]Colgate University, Hamilton, USA

[4]Departament de Química, Universitat Autònoma de Barcelona, Cerdanyola del Vallès, Spain

[5]Molecular Recognition Section, Laboratory of Bioorganic Chemistry, National Institute of Diabetes and Digestive and Kidney Diseases, National Institutes of Health, Bethesda, USA

Abstract

G protein-coupled adenosine receptors are promising therapeutic targets for a wide range of neuropathological conditions, including Parkinson's disease (PD). However, the ubiquity of adenosine receptors and the ultimate lack of selectivity of certain adenosine-based drugs have frequently diminished their therapeutic use. Photopharmacology is a novel approach that allows the spatiotemporal control of receptor function, thus circumventing some of these limitations. Here, we aimed to develop a light-sensitive caged adenosine A_{2A} receptor ($A_{2A}R$) antagonist to photocontrol movement disorders. We synthesized MRS7145 by blocking with coumarin the 5-amino position of the selective $A_{2A}R$ antagonist SCH442416, which could be photoreleased upon violet light illumination (405 nm). First, the light-dependent pharmacological profile of MRS7145 was determined in $A_{2A}R$-expressing cells. Upon photoactivation, MRS7145 precluded $A_{2A}R$ ligand binding and agonist-induced cAMP accumulation. Next, the ability of MRS7145 to block $A_{2A}R$ in a light-dependent manner was assessed *in vivo*. To this end, $A_{2A}R$ antagonist-mediated locomotor activity potentiation was evaluated in brain (striatum) fiber-optic implanted mice. Upon irradiation (405 nm) of the dorsal striatum, MRS7145 induced significant hyperlocomotion and counteracted haloperidol-induced catalepsy and pilocarpine-induced tremor. Finally, its efficacy in reversing motor impairment was evaluated in a PD animal model, namely the hemiparkinsonian 6-hydroxydopamine (6-OHDA)-lesioned mouse. Photo-activated MRS7145 was able to potentiate the number of contralateral rotations induced by L-3,4-dihydroxyphenylalanine (L-DOPA).

Corresponding authors: Kenneth A. Jacobson (kennethj@niddk.nih.gov); Francisco Ciruela (fciruela@ub.edu).

Overall, MRS7145 is a new light-operated $A_{2A}R$ antagonist with potential utility to manage movement disorders, including PD.

Graphical abstract

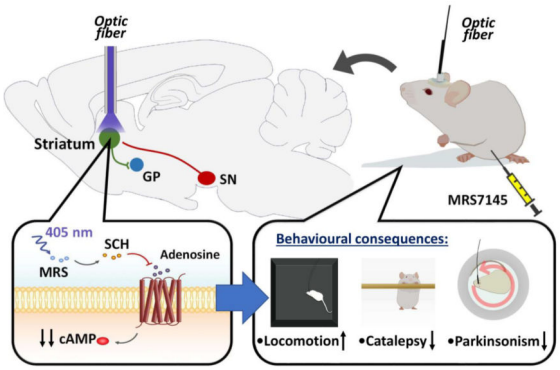

Keywords

Movement disorder; adenosine A_{2A} receptor; photopharmacology; SCH442416; locomotor activity; catalepsy; tremor; Parkinson's disease

1. Introduction

Parkinson's disease (PD) is the second most common neurodegenerative disorder after Alzheimer disease [1]. Its pathological hallmark involves the presence of intracytoplasmic proteinaceous neuronal inclusions in neuronal perikarya and neuronal cell processes known as Lewy bodies (LB). LB formation results in the degeneration of dopamine neurons in substantia nigra pars compacta (SNc), which causes a consequent degeneration of the nigrostriatal dopaminergic pathway leading to a reduction of striatal dopamine levels [2]. The striatum, the main input nuclei of the basal ganglia, receives information from different brain structures, including cortex and thalamus [3]. Neurotransmitters released at the basal ganglia regulate a number of brain functions, such as elicitation and learning of reward- and aversive stimuli-associated behaviors, motor activity control and sensorimotor gating [4,5]. Thus, striatal dopamine, through dopaminergic receptors, plays a central role in motor activity control. Indeed, degeneration of nigrostriatal dopaminergic neurons correlates well with the severe motor impairments shown in PD [1]. Accordingly, common PD pharmacotherapy aims to restore striatal dopaminergic signaling by using the dopamine precursor L-3,4-dihydroxyphenylalanine (L-DOPA). Alternatively, selective dopamine D_2 receptor (D_2R) agonists are used [6]. However, dyskinesia and other adverse effects may accompany chronic D_2R-based therapy [7]. Over the last two decades, alternative non-dopaminergic drugs have been explored to ameliorate these adverse effects, including L-DOPA-induced dyskinesia (LID) [7,8]. Among these novel substances, adenosine A_{2A} receptor ($A_{2A}R$) antagonists emerged as promising antiparkinsonian and antidyskinetic drugs [9,10], and one of them, istradefylline, was recently introduced into clinics in Japan (i.e. Nouriast® tablets, 20 mg) [11]. However, since $A_{2A}Rs$ are expressed throughout the

body, A_{2A}R-based medications may display off-target effects. Thus, A_{2A}R ligands may alter cardiovascular function [12], platelet aggregation [13], thymocyte proliferation [14] or may change hippocampal neuronal activity [15], mood [16] and wakefulness [17]. Overall, the use of A_{2A}R antagonists as antiparkinsonian drugs may trigger undesirable side effects, limiting their clinical use.

The use of optical tools in neuroscience is attracting considerable attention due to the ability to dissect neural circuits with high spatiotemporal resolution [18,19]. Photopharmacology, as distinct from optogenetics, which requires the genetic introduction of light-sensitive proteins (i.e. channels or receptors), uses light-sensitive molecules that modulate endogenous targets upon local irradiation [20,21]. As a consequence, photoactive drugs offer superior tissue specificity and reduced off-target effects [20]. Two types of photosensitive drugs are used in photopharmacology, namely photoswitchable molecules and caged-compounds [20,21]. Previously, we developed a photoisomerizable nonselective adenosine receptor agonist, MRS5543, which behaved as a partial A_{2A}R agonist in the dark (*trans* isomer), while upon blue (i.e. 460 nm) light irradiation it became an antagonist [22]. However, the lack of selectivity and short lifetime (i.e. milliseconds) of the photo-induced *cis* configuration rendered the compound not suitable for *in vivo* A_{2A}R blockade. Therefore, we aimed to overcome these pharmacological or photochemical drawbacks associated with photoswitchable compounds and thus we developed a caged-A_{2A}R antagonist, namely MRS7145, to achieve amenable temporal receptor photocontrol in behaving animals. Interestingly, MRS7145 showed light-dependent A_{2A}R antagonist activity in living cells. In addition, *in vivo* MRS7145 photorelease allowed motor activity control and showed light-dependent antiparkinsonian-like efficacy in mice.

2. Materials and methods

2.1. Synthesis of MRS7145

MRS7145 synthesis is described in detail in the Supplementary Information and supplementary Fig. 1 [23]. All NMR spectral assignments were determined with ^{1}H (400 MHz), ^{13}C (100 MHz) in $CDCl_3$ (Supplementary Fig. 2). Peaks were referenced to residual chloroform signals (δH 7.26 ppm, or δC 77.0 ppm). High resolution mass spectra were recorded on an ESI-TOF instrument.

2.2. Photochemical characterization

To monitor MRS7145 photo-uncaging, a 20 μM solution of this compound in PBS:DMSO 1:1 at 37°C was irradiated at 405 nm and 3 mW with a cw diode laser, and spectral changes were monitored by UV-vis absorption spectroscopy in an UV-vis HP 8453 spectrophotometer (Agilent Technologies, Inc., Colorado Springs, CO, USA). Control experiments were conducted by irradiating SCH442416 (Tocris Bioscience) and 7-diethylamino-4-hydroxymethylcoumarin (Indofine Chemical Co., Hillsborough, NJ) solutions at the same conditions. Photo-uncaging quantum yields were determined using the photoisomerization process of *trans*-azobenzene in acetonitrile as a reference and following the methodology described [24].

2.3. Cell culture and stable transfection

Human embryonic kidney (HEK)-293T cells were grown in Dulbecco's modified Eagle's medium (DMEM) (Sigma-Aldrich, St. Louis, MO, USA) supplemented with 1 mM sodium pyruvate, 2 mM L-glutamine, 100 U/mL streptomycin, 100 mg/mL penicillin and 5% (v/v) fetal bovine serum at 37°C and in an atmosphere of 5% CO2. HEK-293 cells growing in 60 cm^2 plates were transfected with the cDNA encoding the CFP-tagged human $A_{2A}R$ ($A_{2A}R^{CFP}$) [25] using TransFectin™ Lipid Reagent (Bio-Rad Laboratories, Hercules, CA, USA). Fluorescent cells were selected every 2 weeks for 2 months using a Cell sorter (MoFlo Astrios, Beckman Coulter) to enrich the percentage of cells that express the receptor, thus ensuring its permanent expression.

2.4. Synthesis of MRS5842

The fluorescent dye Alexa-647 was covalently attached to the $A_{2A}R$ agonist 2-[[2-[4-[2-(2-aminoethyl)-aminocarbonyl]ethyl]phenyl]ethylamino]-5′-N-ethyl-carboxamidoadenosine (APEC) to generate the MRS5842 or $APEC^{647}$, which was purified by HPLC. The synthesis is described in detail in the Supporting Information (Supplementary Fig. 1 and 2)

2.5. Flow cytometry competition binding assays

Receptor binding studies were performed in HEK-293T cells permanently expressing $A_{2A}R^{CFP}$ using the $APEC^{647}$ as previously described [26]. In brief, cells were detached with accutase (Sigma-Aldrich) and resuspended in Hank's balanced salt solution (HBSS) containing 1 mg/ml glucose and 0.1% BSA. Cells (8×10^5 cells/200μl) were firstly incubated with vehicle, MRS7145 (1 μM) or SCH442416 (1 μM, Tocris Bioscience) in silicone-coated reaction vessels and irradiated at 405 nm with a LED (Doric Connectorized LED, Doric Lenses Inc., Quebec, Canada) using an optic fiber (MFP_400/440/900-0.53_0.5m_FC-SMC, Doric Lenses Inc) or mock manipulated (dark) for 5 min. The 405 nm light pulses lasted 500 ms each and were administered at 23 mW output power and 1 Hz frequency. After 5 min, post-irradiated cells were incubated with $APEC^{647}$ (100 nM) during 60 min at 22°C and used directly for flow cytometric measurements. For each binding condition tested, 2×10^4 cells were analyzed using a FACSCanto™ flow cytometer (Becton Dickinson, Heidelberg, Germany) with excitation at 633 nm (red laser) and emission at 660/20 nm. Samples were maintained in the dark during the analysis to avoid photobleaching. Fluorescence events were obtained in the FL-1 channel (Supplementary Fig. 5). Data were collected using Cell Quest Pro software (BD, Franklin Lakes, NJ) and analyzed by GraphPad Prism 6.01 (GraphPad Software, La Jolla, CA, USA).

2.6. cAMP accumulation inhibition assay

cAMP accumulation was measured using the LANCE Ultra cAMP kit (PerkinElmer, Waltham, MA, USA) as previously described [27]. In brief, $A_{2A}R$ HEK-293T cells were detached with accutase (Sigma-Aldrich) and incubated for 1 h at 22°C in Dulbecco's modified Eagle's medium (DMEM) (Sigma-Aldrich) supplemented with 0.1% BSA, adenosine deaminase (ADA, 0.5 U/ml; Roche Diagnostics, GmbH, Mannheim, Germany) and Zardaverin (100 μM; Calbiochem, San Diego, CA, USA). Cells (1×10^4 cells/200μl) were firstly incubated with vehicle or MRS7145 (10 μM or increasing concentrations) and

then irradiated as above indicated. After 5 min, post-irradiated cells were incubated with CGS21680 (10 nM or increasing concentrations) during 30 min at 22°C. Eu-cAMP tracer and ULight™-anti-cAMP reagents were prepared and added to the sample following manufacturer's instructions. The 384-wells plate was incubated 1 h at 22°C in the dark and was then read on a POLARstar microplate reader (BMG Labtech, Durham, NC, USA). Measurements at 620 nm and 665 nm were used to detect the TR-FRET signal and the concomitant cAMP levels were calculated following manufacturer's instructions. Data were fitted by non-linear regression using GraphPad Prism 6.01.

2.7. Immunohistochemistry

Mice were anesthetized and intracardially perfused with 100 ml of ice-cold 4% paraformaldehyde (PFA) in phosphate buffered saline (PBS; 8.07 mM Na_2HPO_4, 1.47 mM KH_2PO_4, 137 mM NaCl, 0.27 mM KCl, pH 7.2). Brains were post-fixed overnight in the same solution of PFA at 4°C. Coronal sections (50 μm) were obtained using a vibratome (Leica Lasertechnik GmbH, Heidelberg, Germany). Slices were collected in Walter's antifreezing solution (30% glycerol, 30% ethylene glycol in PBS, pH 7.2) and kept at −20°C until processing. For immunohistochemistry of brain slices, these were washed three times with PBS, permeabilized with 0.5% Triton X-100 in PBS for 2 h and rinsed again three times with washing solution (0.05% Triton X-100 in PBS). The slices were then incubated with washing solution containing 10% normal donkey serum (NDS; Jackson ImmunoResearch Laboratories, Inc., West Grove, PA, USA) for 2 h at room temperature. Subsequently, slices were incubated with rabbit anti-TH (3 μg/ml; Millipore, Billerica, MA, USA) or goat anti-$A_{2A}R$ (3 μg/ml; Santa Cruz Biotechnology, Dallas, TX, USA) in washing solution containing 10% NDS for 48h at 4°C. Next, slices were washed with washing solution containing 1% NDS before the incubation with Cy2-conjugated donkey anti-rabbit or anti-goat IgG antibody (1:200; Jackson ImmunoResearch Laboratories, West Grove, PA, USA) in washing solution for 2 h at room temperature. Finally, slices were washed twice with washing solution containing 1% NDS and then mounted with Vectashield immunofluorescence medium (Vector Laboratories, Peterborough, UK) in glass slides. Fluorescence striatal images were captured using a Leica TCS 4D confocal scanning laser microscope (Leica Lasertechnik GmbH).

2.8. Animals

CD-1 mice (animal facility of University of Barcelona) at 5 weeks of age were used. The University of Barcelona Committee on Animal Use and Care approved the protocols. Animals were housed and tested in compliance with the guidelines described in the Guide for the Care and Use of Laboratory Animals [28] and following the European Union directives (2010/63/EU). All efforts were made to minimize animal suffering and the number of animals used. Animals were housed in groups of five in standard cages with *ad-libitum* access to food and water and maintained under controlled standard conditions (12 h dark/light cycle starting at 7:30 AM, 22°C temperature and 66% humidity).

2.9. Brain optic fiber implantation

Mice were anesthetized by administering (intraperitoneally, i.p.) a mixture of ketamine (100 mg/kg, Merial, Spain)/xylazine (10 mg/kg, Calier, Spain). Optical fibers

(TFC_400/475-0.53_3.0mm_TSM4.0_B45 or MFC_400/475-0.53_2.5mm_TSM4.0_B45, Doric Lenses Inc) were stereotaxically (Kopf Instruments, Tujunga, USA) implanted at coordinates: i) AP=+0.5, ML=±2.0, DV=−3.0 for the TFC (Two Ferrule Cannule) and; ii) AP=+0.5, ML=+2.0, DV=−2.5 for MFC (Mono Ferrule Cannule), following to the atlas of Paxinos and Franklin [29] (Supplementary Fig. 7B and C). Chirurgic steel anchor screws 2 mm long with a thread of 1 mm O.D. (Agnthos, Lidingö, Sweden) were used. Screws were placed at AP=−3.0, ML=±2.0 and predrilled holes were made with a 0.7 mm drill bit. Finally, a plastic ring was placed to the skull to encompass optical fibers and screws. The ring was filled with dental cement (DENTALON plus, Heraeus Kulzer GmbH, Germany) to embrace all the elements together. After optic fiber implantation mice were treated with Meloxicam (1 mg/kg, Boehringer Ingelheim, Germany) for three days and they were checked routinely for one week.

2.10. Locomotor activity tests

The open field test was used to evaluate the spontaneous or drug-induced locomotor activity in TFC-implanted CD-1 mice. In brief, animals were administered (i.p.) with MRS7145 (3 mg/kg), SCH442416 (3 mg/kg, Tocris Bioscience) or vehicle-saline with 5% DMSO and 5% Tween-20 min before the testing session. Non-habituated mice were placed in the center of an activity field arena (30 × 30 cm, surrounded by four 50 cm-high black painted walls) equipped with a camera above to record activity and connected to the light source. Animals were either irradiated with a LED-based fiber optic system (Doric Lenses Inc) at 405nm light or mock manipulated (dark) for 20 min during the testing session. The 405 nm light pulses lasted 500 ms each and were administered at 23 mW output power and 1 Hz frequency. The exploratory behavior of the animals was monitored during a 30-min period. The total distance travelled was analyzed using Spot tracker function from Image J (NIH).

2.11. Catalepsy test

Catalepsy was induced in TFC-implanted CD-1 mice by the administration (i.p.) of haloperidol (1 mg/kg; Tocris Biosciences, Bristol, UK). After one h, haloperidol-induced catalepsy was measured as the duration in seconds of an abnormal upright posture in which the forepaws of the mouse were placed on a horizontal wooden bar (0.6 cm of diameter) that was located 4.5 cm above the floor. Subsequently, mice were administered (i.p.) with either vehicle (i.e. saline with 5% DMSO and 5% Tween), SCH442416 (3 mg/kg, Tocris Bioscience) or MRS7145 (3 mg/kg). After 20 min, animals were irradiated at 405 nm following the above indicated light protocol, and a second haloperidol-induced catalepsy measurement was performed.

2.12. Tremulous Jaw Movements

Mice were administered (i.p.) with either vehicle (i.e. saline containing 5% DMSO and 5% Tween), SCH442416 (3 mg/kg, Tocris Bioscience) or MRS7145 (3 mg/kg). After 20 min, animals were irradiated at 405 nm following the above indicated light protocol. Subsequently, tremulous jaw movements (TJMs) were induced by the administration (i.p.) of pilocarpine (1 mg/kg; Sigma-Aldrich). Mice were placed in the observation chamber (i.e. 14.4 × 7.6 × 7 cm clear glass chamber elevated 40 cm from the floor) and allowed 10 min to habituate before TJMs were recorded for 10 min. TJMs were defined as rapid vertical

deflections of the lower jaw that resembled chewing but were not directed at any particular stimulus [30].

2.13. 6-Hydroxydopamine lesion

6-Hydroxydopamine (6-OHDA) lesion was performed as previously described [25]. Briefly, two-month old mice were anesthetized (see above) and one microliter of freshly prepared 6-OHDA solution (3.2 mg/ml free base in 0.02% ascorbate-saline) was stereotaxically (Kopf Instruments) injected at the medial forebrain bundle (MFB) using the following coordinates: AP=−1.2, ML=−1.3, DV=−4.7 (Supplementary Fig. 7A and C). The injections were performed at a rate of 0.5 μl/min using a 10-μl Hamilton syringe. The Hamilton syringe was left in place for 2 min before and 2 min after the injection. After surgery, mice were treated with Meloxicam (1 mg/kg, Boehringer Ingelheim, Germany) for three days and they were checked routinely for one week. Three weeks after the lesion, the extent of dopamine deafferentation was validated by assessing the rotating behavioral response to apomorphine administration. In brief, mice were injected with apomorphine (3 mg/kg, i.p.; Sigma-Aldrich) and the number of full contralateral turns recorded during a 1 h period. Dopamine depletion was considered successful in those animals that made at least 200 net contralateral rotations. Thereafter, an optic fiber (MFC) was implanted in animals with higher scores in a second operation as described above. Finally, animals were housed during three weeks before use.

2.14. Rotational test

6-OHDA lesioned animals were treated (i.p.) with benserazide hydrochloride (25 mg/kg; Sigma-Aldrich), L-DOPA methyl ester (submaximal dose: 4 mg/kg; Sigma-Aldrich) and either vehicle, MRS7145 (3 mg/kg) or SCH442416 (3 mg/kg, Tocris Bioscience). After 10 min, animals were placed in a white cylinder (30 × 10 cm diameter) equipped with a camera above and connected to the light source. Animals were irradiated with a LED-based fiber optic system (Doric Lenses Inc.) at 405 nm or mock manipulated (dark) for 20 min during the testing session. The 405 nm light pulses lasted 500 ms each and were administered at 23 mW output power and 1 Hz frequency. The rotational behavior of animals was monitored during a 40-min period. Each 360° clock-wise or counter clock-wise turn was manually counted from the movie generated.

2.15. Statistical analysis

The number of samples or animals (n) for each set of experiments is indicated in the figure legends. Statistical analysis was performed by one-way ANOVA with Tukey multiple comparison test or Student's *t*-test when appropriate. Statistical significance was considered at $P < 0.05$.

3. Results

3.1. Design and synthesis of a caged $A_{2A}R$ antagonist

The $A_{2A}R$-based ligand MRS7145 was synthesized (Supplementary Fig. 1 and 2) by modifying the amino group of SCH442416, a selective $A_{2A}R$ antagonist [31], to generate a carbamate derivative containing violet light-absorbing coumarin (Fig. 1A). Subsequently, we

characterized MRS7145 photochemically. The UV-vis absorption spectrum of MRS7145 showed signals arising from its two different building blocks: a peak at *ca.* 265 nm, which fit well the absorption maximum found for SCH442416, and another band at *ca.* 385 nm corresponding to the coumarin unit (7-diethylamino-4-hydroxymethylcoumarin, Fig. 1B). The photochemical behavior of MRS7145 was then explored upon selective coumarin excitation at 405 nm. This wavelength was chosen based on previous results showing its safety and efficacy for *in vivo* uncaging [32]. Indeed, whereas no photodegradation of SCH442416 and the separated coumarin chromophore was observed under these irradiation conditions (Supplementary Fig. 4), spectral changes were registered for MRS7145 that are consistent with the photolysis of the coumarin benzylic bond and the release of the appended SCH442416 fragment [32] (Fig. 1C). A photo-uncaging quantum yield of $\Phi_{chem} = 0.01$ was determined for this process, which is in fair agreement with the photochemical behavior reported for other biologically-active pyrimidine derivatives caged with 7-diethylamino-4-hydroxymethylcoumarin [33,34].

3.2. Optical control of $A_{2A}R$ function in cultured cells

We assessed the light-dependent MRS7145-mediated $A_{2A}R$ blockade by using a new fluorescent ligand binding assay and classical cAMP accumulation experiments in cells expressing $A_{2A}R$. First, a new $A_{2A}R$ fluorescent agonist (i.e. APEC^{647}) (Supplementary Fig. 3) was synthesized and used in a flow cytometry-based ligand binding assay [26]. The characterization of APEC^{647} binding to $A_{2A}R$ expressed in HEK-293T cells (Fig. 2A) revealed a dissociation constant within the nanomolar range ($K_d = 20 \pm 5$ nM) (Supplementary Fig. 5). We then performed displacement experiments of APEC^{647} with SCH442416 and MRS7145 in the absence and presence of light. As expected, SCH442416 fully displaced bound APEC^{647} regardless of the illumination conditions (Fig. 2B), while MRS7145 displaced bound APEC^{647} only upon 405 nm cell irradiation (Fig. 2B), thus demonstrating its light-dependent activity. Next, we assessed the light-dependent MRS7145-mediated modulation of cAMP accumulation induced by $A_{2A}R$ activation. To this end, increasing concentrations of a prototypical $A_{2A}R$ full agonist (i.e. CGS21680) were incubated in the absence or presence of MRS7145 and under different irradiation conditions (Fig. 2C). In the dark, CGS21680 induced a dose-dependent increase of cAMP accumulation with low nanomolar potency both in saline- and MRS7145-treated cells ($pEC_{50} = 9.2 \pm 0.1$ and $pEC_{50} = 8.6 \pm 0.1$, respectively) and with comparable efficacy (Fig. 2C). Conversely, while light neither affected potency nor efficacy of saline-treated cells (data not shown), 405 nm irradiation of MRS7145-incubated cells abolished CGS21680-induced cAMP accumulation (Fig. 2C). In addition, MRS7145 was able to preclude $A_{2A}R$-mediated cAMP accumulation in a light- and dose-dependent manner ($pEC_{50} = 8.3 \pm 0.1$) (Fig. 2D). Overall, these results revealed a low nanomolar potency for the light-dependent MRS7145-mediated $A_{2A}R$ blockade in cultured cells.

3.3. Light-dependent efficacy of MRS7145 in animal models of movement disorders

Once MRS7145 light-dependent activity was validated in living cells, we aimed to assess its efficacy in animal behavior. We first evaluated the impact of striatal MRS7145 uncaging in the spontaneous locomotor activity of mice. To this end, a dual fiber-optic cannula was implanted in the dorsal striatum (Fig. 3A), and spontaneous locomotion assessed after

administration (i.p.) of vehicle, SCH442416 or MRS7145, in the absence and presence of light (405 nm) (Fig. 3B). SCH442416 produced a significant increase in the spontaneous locomotor activity of freely moving animals, regardless the illumination paradigm (Fig. 3B and C). Importantly, while MRS7145 did not alter spontaneous locomotion in non-irradiated mice, it significantly ($P < 0.001$) increased locomotor activity upon 405 nm light striatal irradiation (Fig. 3B and C). Coumarin alone did not have any effect on spontaneous locomotion at any dose tested (0.5-6.0 mg/kg) (Supplementary Fig. 6). Overall, these results demonstrated the ability to uncage (at 405 nm) MRS7145 in the dorsal striatum of mice, and to manipulate the spontaneous locomotor activity of freely moving animals.

Next, we assessed the *in vivo* light-dependent efficacy of MRS7145 in two animal models that mimic two PD symptoms, namely rigidity and tremor. We first evaluated the light-dependent effects of MRS7145 on haloperidol-induced catalepsy. While SCH442416 showed a light independent anticataleptic activity (Fig. 3D), as expected [35], MRS7145 was only able to reverse haloperidol-induced catalepsy upon 405 nm light striatal irradiation (Fig. 3D). Next, we evaluated the efficacy of MRS7145 to counteract pilocarpine-induced tremulous jaw movement (TJM). Again, SCH442416 showed a light-independent antitremulous activity (Fig. 3E), as previously reported [36]. And similarly, MRS7145 was unable to reverse TJM in dark conditions, while it fully blocked ($P < 0.001$) pilocarpine-induced TJM upon 405 nm light striatal irradiation (Fig. 3E). Overall, these results demonstrated the efficacy of striatal MRS7145 photo-uncaging in animal models of movement disorders.

3.4. Light-dependent antiparkinsonian-like efficacy of MRS7145

To reinforce the notion that MRS7145 photo-uncaging in the dorsal striatum would be a valuable approach for PD treatment, we evaluated the effects of MRS7145 in the unilateral 6-hydroxydopamine (6-OHDA)-lesioned mouse PD model. To this end, we lesioned the medial forebrain bundle (MFB) of the right hemisphere (Supplementary Fig. 7A and C), as previously described [25]. Mice showing significant dopamine denervation (see Materials and Methods) underwent surgery to implant a single optical fiber at the 6-OHDA lesioned hemisphere (Fig. 4A). As expected for $A_{2A}R$ antagonists [37], SCH442416 potentiated the contralateral rotations induced by a submaximal L-DOPA dose (4 mg/kg) (Fig. 4B). This antiparkinsonian-like activity of SCH442416 was unaffected by 405 nm light hemi-irradiation. On the other hand, MRS7145 was unable to potentiate L-DOPA-induced contralateral rotations in dark conditions; while, upon irradiation, it significantly ($P < 0.05$) enhanced the rotational behavior of the hemiparkinsonian mice (Fig. 4B and Video 1). Overall, these results demonstrated a MRS7145 light-dependent antiparkinsonian-like efficacy, thus revealing the ability to photo-control $A_{2A}R$ function in the dorsal striatum.

4. Discussion

The findings reported in the present study provide compelling evidence regarding: i) the feasibility of remotely controlling $A_{2A}R$ function *in vivo*, and ii) the putative usefulness of photo-active drugs in the management of movement disorders. To our knowledge, MRS7145 is the first compound able to block $A_{2A}R$ in a light-dependent manner, not only in living

cells, but also in behaving animals. Accordingly, MRS7145 photoactivation with violet light precluded $A_{2A}R$ signaling in cultured cells, while photo-uncaging in the mice dorsal striatum prompted hyperlocomotion, counteracted haloperidol-induced catalepsy and pilocarpine-induced tremor, and reversed motor impairments in a PD model.

It has been clinically demonstrated that $A_{2A}R$ antagonists are effective in improving PD motor dysfunction, both in monotherapy [38] and in combination with L-DOPA or other antiparkinsonian drugs [39]. However, further clinical development has been compromised, in part due to the ubiquity of $A_{2A}R$, which may produce some mild to severe adverse antagonist effects, including insomnia, headache, constipation, hallucinations, asthma, infection, urosepsis or cardiac failure [37,40]. Indeed, classical pharmacology displays some important drawbacks: i) slow and imprecise drug delivery; ii) low specificity (i.e. drugs producing more than one effect); and iii) effects are non-resolved, either in space or time (i.e. drugs are usually active in every tissue they reach, until they are degraded or eliminated). The optical control of $A_{2A}R$ with photosensitive antagonists (i.e. MRS7145) may provide enough spatiotemporal resolution to circumvent these drawbacks, limiting off-target effects, and also allowing to locally adjust dosage. In addition, the use of light may permit mapping $A_{2A}R$ function, not only in the striatum but also in other brain regions (i.e. cortex, hippocampus, thalamus), thus contributing to dissect the adenosinergic system circuitry within the brain. Indeed, it may help to understand the presence of extrastriatal $A_{2A}R$, which could have opposing functions to striatal $A_{2A}R$, as recently demonstrated [41]. Overall, our data support that MRS7145-based spatiotemporal $A_{2A}R$ manipulation may contribute not only to the mechanistic understanding of the brain adenosinergic system, but it also may permit exploring photo-dependent approaches, leading to a better management of movement disorders.

Using light for pharmacological applications (i.e. photopharmacology) might represent a way to circumvent some classical pharmacological shortcomings. However, the irradiation of a tissue non-naturally exposed to light might possibly induce some damage. The majority of photoactivable compounds already used in biology require potentially harmful UV radiation [42], which also displays a poor tissue penetration depth. Consequently, current photocaged compounds are unacceptable for *in vivo* and clinical use and are limited to *in vitro* applications. Here, we designed and synthesized a selective photocaged $A_{2A}R$ antagonist with effective *in vitro* and *in vivo* uncaging at 405 nm (visible spectrum), which upon exposure to a specific irradiation protocol was shown to be non-toxic for neurons [32]. On the other hand, the use of photocaged compounds to modify neuronal activity may provide some advantages over other related approaches, namely optogenetics and deep brain stimulation (DBS). Unlike optogenetics, photopharmacology does not require viral-mediated gene delivery of photosensitive proteins, thus avoiding certain ethical considerations. In addition, optogenetics does not allow the direct blockade of a specific endogenous receptor, whereas photopharmacology permits both agonism and antagonism activity assessment. DBS has a great temporal resolution, but it displays two major drawbacks, namely a lack of cell-type specificity and electrode-glia encapsulation. First, glial cells increase impedance and demand high—electrical currents to reach the desired areas, which leads to a lower spatial resolution of DBS than that exhibited by caged compounds. In addition, glia encapsulation is a major problem associated with DBS. It may also affect optical fibers but

to a lesser extent, since glial cells are optically transparent [43]. Finally, it is important to note that one important drawback of photocaged compounds (i.e. MRS7145) would be their irreversible nature. In this sense, the design and development of novel photoswitchable compounds with high selectivity and longer lifetimes may permit a better temporal resolution. In addition, the development of novel wireless optical fibers, which have been already designed and tested [44], may enable a substantial growth of photopharmacology in the near future.

5. Conclusions

Action of conventional drugs is often limited by a lack of temporal and site specificity, leading to side effects that can impede their clinical development. Photopharmacology combines the power of light and pharmacology for spatiotemporal resolution of drug action *in vivo*, thus limiting off-target effects and allowing local dose adjustments. Here, we developed the first adenosine A_{2A} receptor antagonist endowed with light-dependent activity.

In conclusion, MRS7145 is the first photo-controlled A_{2A}R antagonist capable of binding and blocking A_{2A}R in a light-dependent fashion in living cells. Upon local brain irradiation, MRS7145 allows the fine control of spontaneous locomotor activity and reversal of pharmacologically-induced Parkinsonian-like behavior. Our data demonstrate that this compound can be effectively photo-delivered in the striatum of rodents, increasing locomotor activity while reverting pharmacologically-induced parkinsonian-like symptoms. Our results constitute a proof of concept to design novel approaches for movement disorder management.

Supplementary Material

Refer to Web version on PubMed Central for supplementary material.

Acknowledgements

This work was supported by MINECO/ISCIII (SAF2017-87349-R and PIE14/00034), the Catalan government (2017 SGR 1604), Fundació la Marató de TV3 (Grant 20152031), FWO (SBO-140028) to FC, NIDDK Intramural Research Program (ZIADK031117) to KJ and MINECO/FEDER (CTQ2015-65439-R) to JH. We thank to Esther Castaño and Benjamín Torrejón, from the CCiT-Bellvitge Campus of the University of Barcelona, for the technical assistance.

References

[1]. Poewe W, Mahlknecht P. The clinical progression of Parkinson’s disease. Parkinsonism & Related Disorders. 2009; 15(Suppl 4):S28–32. DOI: 10.1016/S1353-8020(09)70831-4 [PubMed: 20123553]

[2]. Cookson MR. The biochemistry of Parkinson’s disease. Annual Review of Biochemistry. 2005; 74:29–52. DOI: 10.1146/annurev.biochem.74.082803.133400

[3]. Gerfen CR, Wilson CJ. The basal ganglia. In: Swanson LW, Björklund A, Hökfelt T, editorsHandbook of Chemical Neuroanatomy. Elsevier; Amsterdam: 1996. 371–468.

[4]. Swerdlow NR, Geyer MA, Braff DL. Neural circuit regulation of prepulse inhibition of startle in the rat: Current knowledge and future challenges. Psychopharmacology. 2001; 156:194–215. DOI: 10.1007/s002130100799 [PubMed: 11549223]

[5]. Bromberg-Martin ES, Hikosaka O, Nakamura K. Coding of Task Reward Value in the Dorsal Raphe Nucleus. Journal of Neuroscience. 2010; 30:6262–6272. DOI: 10.1523/JNEUROSCI.0015-10.2010 [PubMed: 20445052]

[6]. Romrell J, Fernandez HH, Okun MS. Rationale for current therapies in Parkinson's disease. Expert Opinion on Pharmacotherapy. 2003; 4:1747–61. DOI: 10.1517/14656566.4.10.1747 [PubMed: 14521485]

[7]. Huot P, Johnston TH, Koprich JB, Fox SH, Brotchie JM. The pharmacology of L-DOPA-induced dyskinesia in Parkinson's disease. Pharmacological Reviews. 2013; 65:171–222. DOI: 10.1124/pr.111.005678 [PubMed: 23319549]

[8]. Fox SH, Brotchie JM, Lang AE. Non-dopaminergic treatments in development for Parkinson's disease. Lancet Neurology. 2008; 7:927–938. DOI: 10.1016/S1474-4422(08)70214-X [PubMed: 18848312]

[9]. Grondin R, Bedard PJ, Hadj Tahar A, Gregoire L, Mori A, Kase H. Antiparkinsonian effect of a new selective adenosine A_{2A} receptor antagonist in MPTP-treated monkeys. Neurology. 1999; 52:1673–1677. [PubMed: 10331698]

[10]. Bara-Jimenez W, Sherzai A, Dimitrova T, Favit A, Bibbiani F, Gillespie M, Morris MJ, Mouradian MM, Chase TN. Adenosine A_{2A} receptor antagonist treatment of Parkinson's disease. Neurology. 2003; 61:293–296. [PubMed: 12913186]

[11]. Müller T. The safety of istradefylline for the treatment of Parkinson's disease. Expert Opinion on Drug Safety. 2015; 14:769–75. DOI: 10.1517/14740338.2015.1014798 [PubMed: 25676023]

[12]. Thomas T, St Lambert JH, Dashwood MR, Spyer KM. Localization and action of adenosine A_{2A} receptors in regions of the brainstem important in cardiovascular control. Neuroscience. 2000; 95:513–8. [accessed January 26, 2018] http://www.ncbi.nlm.nih.gov/pubmed/10658631. [PubMed: 10658631]

[13]. Varani K, Portaluppi F, Gessi S, Merighi S, Ongini E, Belardinelli L, Borea PA. Dose and time effects of caffeine intake on human platelet adenosine A_{2A} receptors : functional and biochemical aspects. Circulation. 2000; 102:285–9. [accessed March 31, 2014] http://www.ncbi.nlm.nih.gov/pubmed/10899090. [PubMed: 10899090]

[14]. Apasov SG, Chen J-F, Smith PT, Schwarzschild MA, Fink JS, Sitkovsky MV. Study of A 2A adenosine receptor gene deficient mice reveals that adenosine analogue CGS 21680 possesses no A 2A receptor-unrelated lymphotoxicity. British Journal of Pharmacology. 2000; 131:43–50. DOI: 10.1038/sj.bjp.0703532 [PubMed: 10960067]

[15]. Cunha RA, Milusheva E, Vizi ES, Ribeiro JA, Sebastiao AM. Excitatory and inhibitory effects of A1 and A2A adenosine receptor activation on the electrically evoked [3H]acetylcholine release from different areas of the rat hippocampus. Journal of Neurochemistry. 1994; 63:207–214. [PubMed: 8207430]

[16]. El Yacoubi M, Ledent C, Ménard JF, Parmentier M, Costentin J, Vaugeois JM. The stimulant effects of caffeine on locomotor behaviour in mice are mediated through its blockade of adenosine A_{2A} receptors. British Journal of Pharmacology. 2000; 129:1465–73. DOI: 10.1038/sj.bjp.0703170 [PubMed: 10742303]

[17]. Huang Z-L, Qu W-M, Eguchi N, Chen J-F, Schwarzschild MA, Fredholm BB, Urade Y, Hayaishi O. Adenosine A_{2A}, but not A_1, receptors mediate the arousal effect of caffeine. Nature Neuroscience. 2005; 8:858–859. DOI: 10.1038/nn1491 [PubMed: 15965471]

[18]. Boyden ES. Optogenetics and the future of neuroscience. Nature Neuroscience. 2015; 18:1200–1. DOI: 10.1038/nn.4094 [PubMed: 26308980]

[19]. Song C, Knöpfel T. Optogenetics enlightens neuroscience drug discovery. Nature Reviews: Drug Discoveryeviews. Drug Discovery. 2016; 15:97–109. DOI: 10.1038/nrd.2015.15 [PubMed: 26612666]

[20]. Lerch MM, Hansen MJ, van Dam GM, Szymanski W, Feringa BL. Emerging Targets in Photopharmacology. Angewandte Chemie. 2016; 55:10978–99. DOI: 10.1002/anie.201601931 [PubMed: 27376241]

[21]. Velema WA, Szymanski W, Feringa BL. Photopharmacology: beyond proof of principle. Journal of the American Chemical Society. 2014; 136:2178–91. DOI: 10.1021/ja413063e [PubMed: 24456115]

[22]. Bahamonde MI, Taura J, Paoletta S, Gakh AA, Chakraborty S, Hernando J, Fernández-Dueñas V, Jacobson KA, Gorostiza P, Ciruela F. Photomodulation of G protein-coupled adenosine receptors by a novel light-switchable ligand. Bioconjugate Chemistry. 2014; 25:1847–1854. DOI: 10.1021/bc5003373 [PubMed: 25248077]

[23]. Liu Z, Liu T, Lin Q, Bao C, Zhu L. Photoreleasable thiol chemistry for facile and efficient bioconjugation. Chemical Communications. 2014; 50:1256–8. DOI: 10.1039/c3cc48263d [PubMed: 24336390]

[24]. Lees AJ. A Photochemical Procedure for Determining Reaction Quantum Efficiencies in Systems with Multicomponent Inner Filter Absorbances. Analytical Chemistry. 1996; 68:226–229. DOI: 10.1021/ac9507653 [PubMed: 21619240]

[25]. Fernández-Dueñas V, Gómez-Soler M, López-Cano M, Taura JJ, Ledent C, Watanabe M, Jacobson KA, Vilardaga J-P, Ciruela F. Uncovering Caffeine's Adenosine A_{2A} Receptor Inverse Agonism in Experimental Parkinsonism. ACS Chemical Biology. 2014; 9:2496–501. DOI: 10.1021/cb5005383 [PubMed: 25268872]

[26]. Fernández-Dueñas V, Gomez-Soler M, Morato X, Nunez F, Das A, Kumar TS, Jauma S, Jacobson KA, Ciruela F. Dopamine D2 receptor-mediated modulation of adenosine A_{2A} receptor agonist binding within the $A_{2A}R/D_2R$ oligomer framework. Neurochemistry International. 2013; 63:42–46. DOI: 10.1016/j.neuint.2013.04.006 [PubMed: 23619397]

[27]. Taura J, Fernández-Dueñas V, Ciruela F. Determination of GPCR-mediated cAMP accumulation in rat striatal synaptosomes. Neuromethods. 2016; 110:455–464.

[28]. Clark JD, Gebhart GF, Gonder JC, Keeling ME, Kohn DF. Special Report: The 1996 Guide for the Care and Use of Laboratory Animals. ILAR Journal / National Research Council, Institute of Laboratory Animal Resources. 1997; 38:41–48. [accessed December 8, 2014] http://www.ncbi.nlm.nih.gov/pubmed/11528046.

[29]. Franklin KBJ, Paxinos G. The Mouse Brain in Stereotaxic Coordinates. 3th ed.. Academic Press; 2008.

[30]. Salamone JD, Mayorga AJ, Trevitt JT, Cousins MS, Conlan A, Nawab A. Tremulous jaw movements in rats: a model of parkinsonian tremor. Progress in Neurobiology. 1998; 56:591–611. [accessed July 18, 2014] http://www.ncbi.nlm.nih.gov/pubmed/9871939. [PubMed: 9871939]

[31]. Todde S, Moresco RM, Simonelli P, Baraldi PG, Cacciari B, Spalluto G, Varani K, Monopoli A, Matarrese M, Carpinelli A, Magni F, Kienle MG, Fazio F. Design, radiosynthesis, and biodistribution of a new potent and selective ligand for in vivo imaging of the adenosine A_{2A} receptor system using positron emission tomography. Journal of Medicinal Chemistry. 2000; 43:4359–62. [accessed April 1, 2016] http://www.ncbi.nlm.nih.gov/pubmed/11087559. [PubMed: 11087559]

[32]. Font J, López-Cano M, Notartomaso S, Scarselli P, Di Pietro P, Bresolí-Obach R, Battaglia G, Malhaire F, Rovira X, Catena J, Giraldo J, Pin J-P, Fernández-Dueñas V, Goudet C, Nonell S, Nicoletti F, Llebaria A, Ciruela F. Optical control of pain in vivo with a photoactive mGlu 5 receptor negative allosteric modulator. eLife. 2017; 6:e23545.doi: 10.7554/eLife.23545 [PubMed: 28395733]

[33]. Menge C, Heckel A. Coumarin-caged dG for improved wavelength-selective uncaging of DNA. Organic Letters. 2011; 13:4620–3. DOI: 10.1021/ol201842x [PubMed: 21834506]

[34]. Schönleber RO, Bendig J, Hagen V, Giese B. Rapid photolytic release of cytidine 5'-diphosphate from a coumarin derivative: a new tool for the investigation of ribonucleotide reductases. Bioorganic & Medicinal Chemistry. 2002; 10:97–101. [accessed February 9, 2018] http://www.ncbi.nlm.nih.gov/pubmed/11738611. [PubMed: 11738611]

[35]. Taura J, Valle-León M, Sahlholm K, Watanabe M, Van Craenenbroeck K, Fernández-Dueñas V, Ferré S, Ciruela F. Behavioral control by striatal adenosine A 2A - dopamine D 2 receptor heteromers. Genes, Brain and Behavior. 2017; In press. doi: 10.1111/gbb.12432

[36]. Collins LE, Galtieri DJ, Brennum LT, Sager TN, Hockemeyer J, Müller CE, Hinman JR, Chrobak JJ, Salamone JD. Oral tremor induced by the muscarinic agonist pilocarpine is suppressed by the adenosine A_{2A} antagonists MSX-3 and SCH58261, but not the adenosine A_1 antagonist DPCPX. Pharmacology, Biochemistry and Behavior. 2010; 94:561–9. DOI: 10.1016/j.pbb.2009.11.011

[37]. Pinna A. Adenosine A_{2A} receptor antagonists in Parkinson's disease: progress in clinical trials from the newly approved istradefylline to drugs in early development and those already discontinued. CNS Drugs. 2014; 28:455–74. DOI: 10.1007/s40263-014-0161-7 [PubMed: 24687255]

[38]. Stocchi F, Rascol O, Hauser RA, Huyck S, Tzontcheva A, Capece R, Ho TW, Sklar P, Lines C, Michelson D, Hewitt DJ. Preladenant Early Parkinson Disease Study Group, Randomized trial of preladenant, given as monotherapy, in patients with early Parkinson disease. Neurology. 2017; 88:2198–2206. DOI: 10.1212/WNL.0000000000004003 [PubMed: 28490648]

[39]. Hauser RA, Cantillon M, Pourcher E, Micheli F, Mok V, Onofrj M, Huyck S, Wolski K. Preladenant in patients with Parkinson's disease and motor fluctuations: a phase 2, double-blind, randomised trial. Lancet Neurology. 2011; 10:221–229. DOI: 10.1016/S1474-4422(11)70012-6 [PubMed: 21315654]

[40]. Dungo R, Deeks ED. Istradefylline: First Global Approval. Drugs. 2013; 73:875–882. DOI: 10.1007/s40265-013-0066-7 [PubMed: 23700273]

[41]. Shen H-Y, Coelho JE, Ohtsuka N, Canas PM, Day Y-J, Huang Q-Y, Rebola N, Yu L, Boison D, Cunha RA, Linden J, Tsien JZ, Chen J-F. A critical role of the adenosine A_{2A} receptor in extrastriatal neurons in modulating psychomotor activity as revealed by opposite phenotypes of striatum and forebrain A_{2A} receptor knock-outs. The Journal of Neuroscience. 2008; 28:2970–5. DOI: 10.1523/JNEUROSCI.5255-07.2008 [PubMed: 18354001]

[42]. Ellis-Davies GCR. Caged compounds: photorelease technology for control of cellular chemistry and physiology. Nature Methods. 2007; 4:619–28. DOI: 10.1038/nmeth1072 [PubMed: 17664946]

[43]. Aravanis AM, Wang L-P, Zhang F, Meltzer LA, Mogri MZ, Schneider MB, Deisseroth K. An optical neural interface: in vivo control of rodent motor cortex with integrated fiberoptic and optogenetic technology. Journal of Neural Engineering. 2007; 4:S143–S156. DOI: 10.1088/1741-2560/4/3/S02 [PubMed: 17873414]

[44]. Shin G, Gomez AM, Al-Hasani R, Jeong YR, Kim J, Xie Z, Banks A, Lee SM, Han SY, Yoo CJ, Lee J-L, Lee SH, Kurniawan J, Tureb J, Guo Z, Yoon J, Park S-I, Bang SY, Nam Y, Walicki MC, Samineni VK, Mickle AD, Lee K, Heo SY, McCall JG, Pan T, Wang L, Feng X, Kim T, Kim JK, Li Y, Huang Y, Gereau RW, Ha JS, Bruchas MR, Rogers JA. Flexible Near-Field Wireless Optoelectronics as Subdermal Implants for Broad Applications in Optogenetics. Neuron. 2017; 93:509–521.e3. DOI: 10.1016/j.neuron.2016.12.031 [PubMed: 28132830]

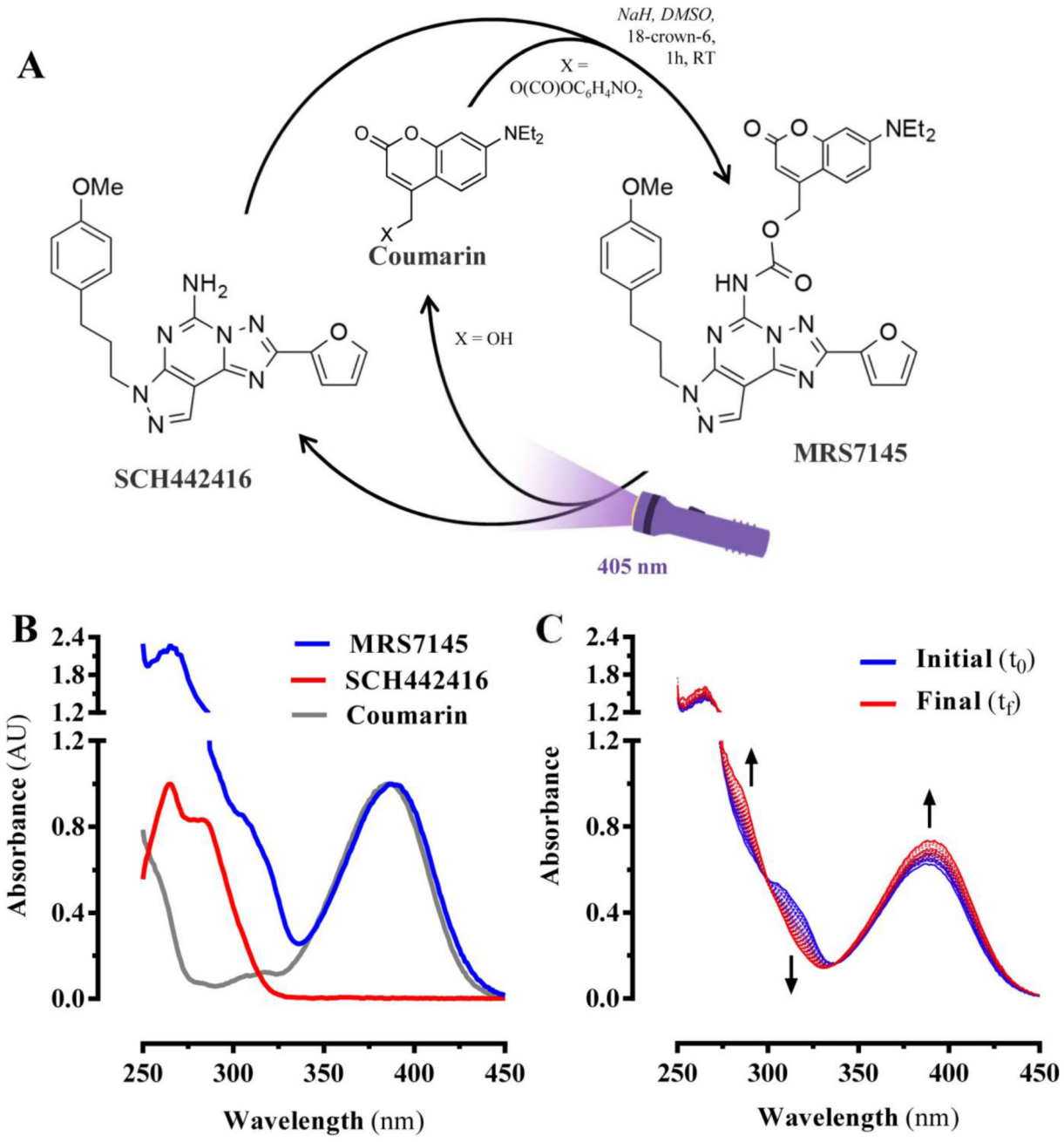

Figure 1. Design, synthesis and photochemical properties of MRS7145

(**A**) The synthesis of MRS7145 involves a procedure using SCH442416 and 7-diethylamino-4-hydroxymethylcoumarin (coumarin). In brief, 60% NaH was first added to a solution of SCH442416 and 18-crown-6. After 15 min, a solution of the coumarin nitrophenyl carbonate was added. After 1 h, DMF was co-evaporated onto SiO_2 with toluene (3 ×) and chromatographed with 20 to 100% EtOAc/hexanes (see Materials and Methods). Upon irradiation with 405 nm visible light the irreversible photolytic reaction produced SCH442416. (**B**) Absorption spectra of 7-diethylamino-4-hydroxymethylcoumarin,

SCH442416 and MRS7145 in PBS:DMSO 1:1 and 37 °C. (**C**) Time-course of spectral changes registered for MRS7145 in PBS:DMSO 1:1 upon irradiation at 405 nm and 37 °C during 30 min, which are consistent with the light-induced uncaging of SCH442416.

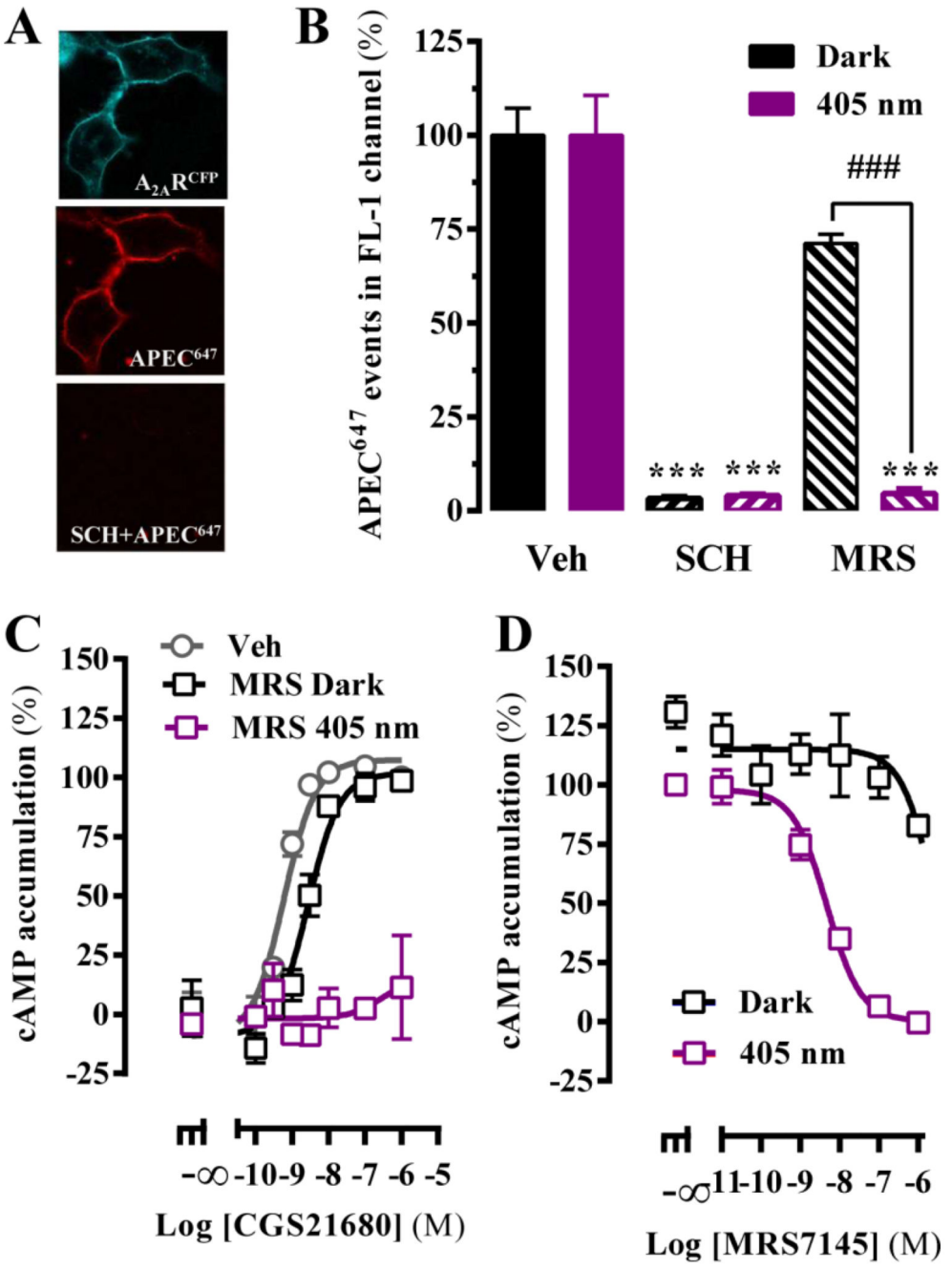

Figure 2. MRS7145-dependent photo-control of exogenously and endogenously expressed adenosine A_{2A} receptor in cultured cells

(**A**) HEK-293 cells stably transfected with the human CFP-tagged adenosine A_{2A} receptor ($A_{2A}R^{CFP}$) were perfused with $APEC^{647}$ (MRS5842) (1 μM) in the absence and presence of SCH442416 (1 μM). (**B**) The binding properties of MRS7145 were measured by a flow cytometer throughout the incubation of $APEC^{647}$ (100 nM) in A_{2A}R-CFP cells in the presence of SCH442416 (1 μM) or MRS7145 (1 μM), all in dark conditions and upon irradiation at 405 nm. Data was expressed as a percentage of the specific events within the

fluorescent region of analysis (Supplementary Fig. 5). The percentage of binding was calculated as described in Materials and Methods and expressed as mean ± SEM (n=4). *P<0.05, ** P < 0.01, *** P < 0.001, **** P < 0.0001, one-way ANOVA with a Tukey's multiple comparison test using the Veh+dark condition as a control. #P<0.05, ## P < 0.01, ### P < 0.001, #### P < 0.0001, Student's t-test when comparing dark vs 405 nm conditions. Similar results were obtained in three independent experiments. (**C**) Determination of A_{2A}R-mediated cAMP accumulation in A_{2A}R-CFP cells. Normalized dose-response of CGS21680-induced cAMP accumulation in the absence (grey circles) or presence of MRS7145 in dark conditions (black squares) and upon irradiation at 405 nm (violet squares) are shown. (**D**) cAMP accumulation in A_{2A}R-CFP cells stimulated with CGS21680 (10 nM) in the absence or presence of increasing concentrations of MRS7145, both in dark conditions (black squares) and upon irradiation at 405 nm (violet squares). The percentage of cAMP accumulation was calculated as described in Materials and Methods and expressed as mean ± SEM (n=3). Similar results were obtained in three independent experiments.

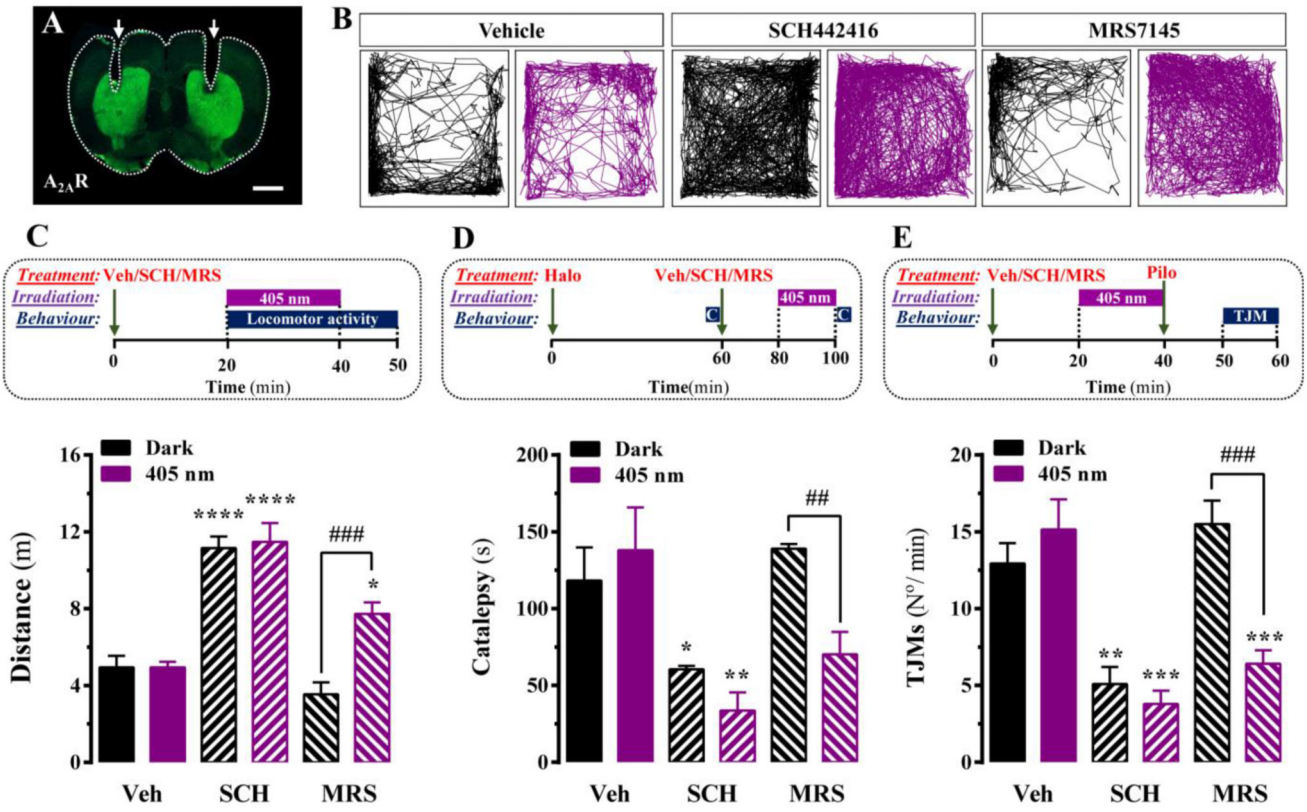

Figure 3. In vivo assessment of MRS7145 light-dependent effect

(**A**) Photomicrographs showing $A_{2A}R$ immunofluorescence staining in a brain coronal sections. The arrows show where the double optic fiber was implanted in the dorsal striatum. (**B**) Representative 30 min trajectories in an open field arena using either Vehicle, SCH442416 or MRS7145 either in dark (black) or 405 nm (violet) conditions. (**C**) Quantification of total horizontal locomotor activity shown in (B) was measured as the total distance travelled. In the upper panel, a scheme of the 405 nm light irradiation protocol (violet rectangles) and open field locomotor activity recordings (blue rectangle) is shown. In brief, animals were administered with vehicle (Veh, i.p.), SCH442416 (SCH, 3 mg/kg, i.p.) or MRS7145 (MRS, 3 mg/kg, i.p.) 20 min before the striatum was irradiated at 405 nm or mock manipulated (dark) for 20 min. Mice were recorded for 30 min, during the irradiation (20 min) and 10 min after. (**D**) Haloperidol-induced cataleptic behaviour was measured as the time spent with both front paws resting on the bar (see Materials and Methods). A cut-off time was set at 200 sec. Animals were intraperitoneally injected with haloperidol (1 mg/kg), and after 1 h either vehicle (Veh, 5% DMSO and 5% Tween-80 in saline), SCH442416 (SCH, 3 mg/kg) or MRS7145 (MRS, 3 mg/kg) were administrated. After 20 min, the striatum was irradiated at 405 nm (or dark) for 20 min. Cataleptic time was measured afterwards. (**E**) Pilocarpine-induced tremulous jaw movements (TJMs) were measured as the number of chewing movements done in 10 min (see Materials and Methods). Animals were intraperitoneally injected with either vehicle (Veh, 5% DMSO and 5% Tween-80 in saline), SCH442416 (SCH, 3 mg/kg) or MRS7145 (MRS, 3 mg/kg) 20 min before the striatum was irradiated at 405 nm (or dark) for 20 min. Pilocarpine (1 mg/kg) was then administrated and

the animal was placed in the observation box for 10 min. The number of purposeless chewing movements were recorded for the last 10 min period using a hand counter. (**C**-**E**) Data (means ± SEM, 5-10 mice per group) over the Veh+dark value. *$P < 0.05$, **$P < 0.01$, ***$P < 0.001$, ****$P < 0.0001$, one-way ANOVA with a Tukey's multiple comparison test using the Veh+dark condition as a control. #$P < 0.05$, ##$P < 0.01$, ###$P < 0.001$, ####$P < 0.0001$, Student's *t*-test when comparing dark vs 405 nm conditions.

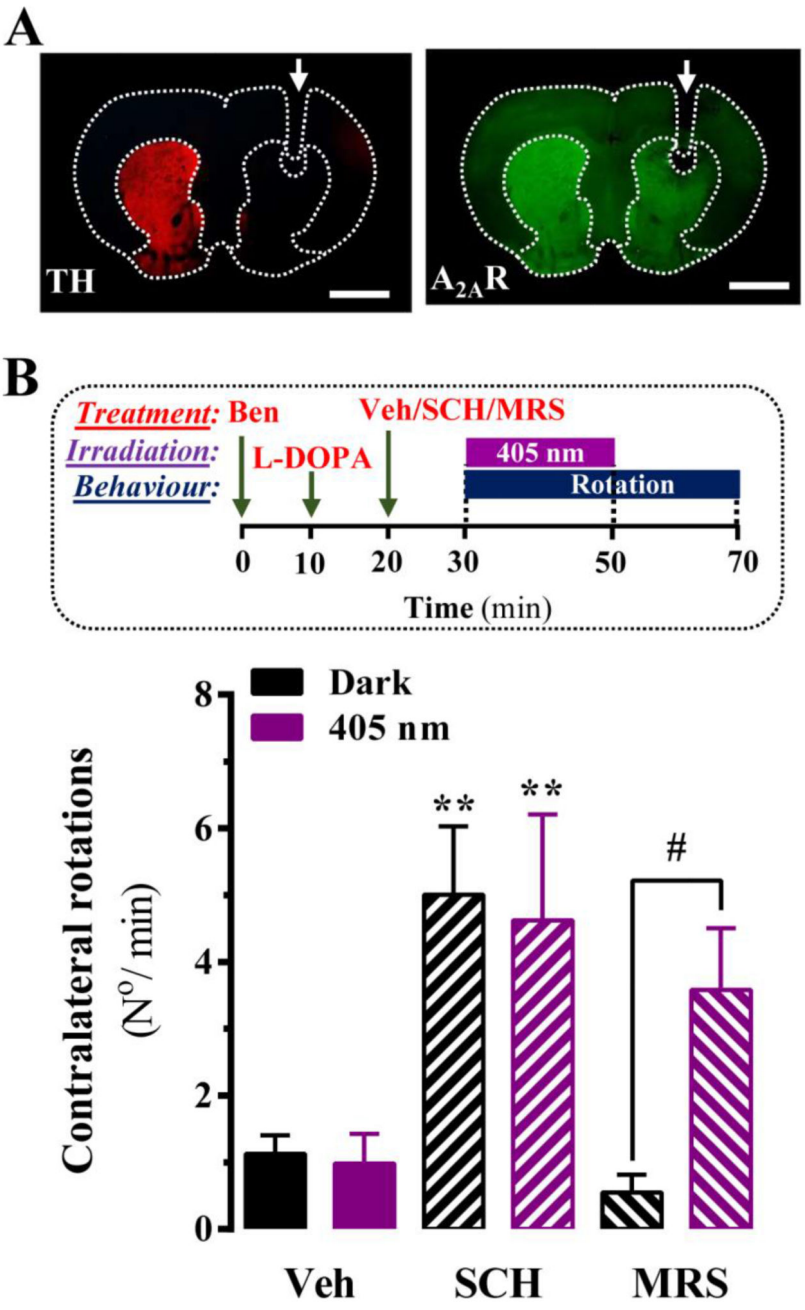

Figure 4. In vivo evaluation of MRS7145 in an optic-fiber implanted and unilateral 6-OHDA-lesioned mouse model

(**A**) Photomicrograph showing tyrosine hydroxylase (TH) and $A_{2A}R$ immunofluorescence staining in brain coronal sections. A loss of dopaminergic innervation in the lesioned (L) compared to the non-lesioned (R) striatum is observed. The arrow indicates where the single optic fiber was implanted. (**B**) MRS7145-mediated potentiation of L-DOPA-induced contralateral rotations were monitored during a 40 min period (see Materials and Methods). Animals were intraperitoneally injected with benserazide (25 mg/kg), followed by a

submaximal dose of L-DOPA (4 mg/kg), and finally injected with either vehicle (Veh, 5% DMSO and 5% Tween-80 in saline), SCH442416 (SCH, 3 mg/kg) or MRS7145 (MRS, 3 mg/kg) 10 min before the right striatum was irradiated at 405 nm (or dark) for 20 min. Data (means ± SEM, 5-10 mice per group) over the Veh+dark value. *P<0.05, ** P < 0.01, *** P < 0.001, **** P < 0.0001, one-way ANOVA with a Tukey's multiple comparison test using the Veh+dark condition as a control. #P<0.05, ## P < 0.01, ### P < 0.001, #### P < 0.0001, Student's t-test when comparing dark vs 405 nm conditions.